

Arctic Ozone **Depletion** observed by UARS MLS during
the 1994-95 Winter

G. L. Manney, L. Froidevaux, J. W. Waters, M. L. Santee,
W. G. Read, D. A. Flower, R.F. Jarnot, R. W. Zurek

Mail Stop 183-701,
Jet Propulsion Laboratory,
California Institute of Technology,
Pasadena, CA 91109, USA.

* To whom correspondence should be addressed.

submitted to Science

The Arctic lower stratosphere was unusually cold and the polar vortex unusually strong throughout the 1994-95 Arctic winter. Upper Atmosphere Research Satellite (UARS) Microwave Limb Sounder (MLS) observations showed enhanced chlorine monoxide (ClO) when viewing high northern latitudes in late December 1994 and again in February and early March 1995. Between late December 1994 and early February 1995, average lower stratospheric ozone in the polar vortex decreased by $\sim 15\%$, with local decreases of $\sim 30\%$; additional local decreases of $\sim 5\%$ were seen between early February and early March. Transport calculations indicate that the ozone decrease is due to chemical processes, as expected from the enhanced ClO. A significant decrease in nitric acid (HNO_3) over the same period indicates some denitrification. The differences between the 1994-95 Arctic winter and the three previous winters observed by MLS demonstrate significant interannual variability in the amount of Arctic ozone depletion; considering projected downward trends in lower stratospheric temperatures, the potential exists for more Arctic ozone depletion in future winters.

The severe ozone depletion over Antarctica(1) in late winter and early spring (the Antarctic "ozone hole") is caused primarily by chlorine chemistry coupled to heterogeneous reactions on the surfaces of polar stratospheric clouds (PSCs) (2). Measurements by UARSMLS during three previous Arctic winters have shown abundances of reactive chlorine in the Arctic polar vortex comparable to those in the Antarctic (3,4,5) and evidence for ozone depletion by chlorine chemistry in the Arctic lower stratosphere (4). Aircraft and ground-based measurements (6) have also shown evidence of Arctic ozone loss in recent years. The amount of ozone loss varied due mainly to interannual variability in the duration, location and extent of temperatures low enough to form PSCs in the Arctic vortex. The Arctic lower stratosphere was unusually and persistently cold in December 1994 and January 1995, and the lower stratospheric vortex was exceptionally strong throughout the 1994-95 winter (7); low temperatures also persisted unusually late, until mid-March 1995. MLS measurements of ozone, chlorine monoxide and nitric acid in late December 1994 and in February and early March 1995 indicated significant chemical ozone depletion and some denitrification by early February.

MLS measurements of microwave emission (8, 9) have provided data on lower stratospheric ClO (3), ozone (3, 4, 5, 10), and HNO₃ (11) for three previous Arctic winters. In the past year, the MLS antenna scanning mechanism (now well past its nominal mission lifetime of 18 months) has developed problems, resulting in degraded temporal and vertical coverage of measurements. From 22 through 30 Dec 1994 and from 1 Feb through 10 Mar 1995, daily MLS measurements are available for one broad pressure layer in the lower stratosphere (12). One full day of three dimensional data from MLS was obtained on 21 Dec 1994. Nine days of three dimensional measurements covering high northern latitudes were obtained in February and early March 1995 (13).

Mixing ratios of HNO₃, ClO and ozone on 21 Dec 1994 and three days when MLS was scanning during the February and March 1995 north-viewing period are shown in Fig. 1, on the 465 K isentropic [constant potential temperature (14)] surface [near 40 hPa (~18 km)

in polar regions). Column ozone above 100 hPa is shown for the same days. Two contours of 465 K PV (15) arc overlaid on the mixing ratio maps, in the region of strong PV gradients which presents a barrier to mixing and thus can be considered an approximate definition of the vortex edge (16, 17). Temperature contours (18) of 190 and 195 K arc overlaid on the HNO₃ maps. Temperatures fell below the type I [nitric acid trihydrate (NAT)] PSC formation threshold (19) (~ 195 K) in early December 1994 (Fig. 2a) and were near or below the type II (water) PSC formation threshold (19) (~ 188 K) from ~ 15 Dec 1994 through ~ 15 Jan 1995. Temperatures in late December 1994 were considerably lower than at the same time in any of the three previous Arctic winters. Although temperatures in early January 1992 and 1993 occasionally dropped to values as low as in January 1995, they did not remain at those low values for more than a few days. The time evolution of MLS ClO and ozone averaged within the vortex is summarized in Fig. 2b [including estimates of vortex-averaged ClO from non-scanning measurements (20)] and 2c, in comparison with measurements from the previous three Arctic winters.

Ozone and HNO₃ abundances were large in the vortex on 21 Dec 1994 (Fig. 1a and 1c). This is consistent with downward transport that was strongest well within the vortex in recent Arctic early winters (16). Fig. 2c shows that 21 Dec 1994 vortex-averaged ozone was near to or slightly lower than values at that time in the previous three years. Maximum HNO₃ values were slightly lower than those shown by Santec et al. (11) for early December 1992. Lower values of ozone and HNO₃ than in previous years suggest weaker diabatic descent, which would be consistent with the colder early winter (16).

A cavity was apparent in HNO₃ on 21 Dec 1994, coincident with the region of lowest temperatures. At temperatures near the type I PSC formation threshold, ~ 10 ppbv of gaseous HNO₃ can coexist with NAT; however, as temperatures drop this is no longer the case, and most of the HNO₃ is sequestered in PSCs at temperatures below ~ 192 K (21). Since MLS measures only gaseous HNO₃, the depression in HNO₃ on 21 Dec 1994 indicates sequestration in PSCs. Non-scanning MLS HNO₃ measurements for 22 through 30 Dec 1994

showed a cavity indicating that HNO_3 was mainly condensed in PSCs. The cavity deepened until about 26 Dec 1994, and then became less pronounced when temperatures increased (Fig. 2a). This temporary depression is thus evidence for the presence of PSCs, rather than for irreversible removal of HNO_3 (denitrification). ClO on 21 Dec 1994 was enhanced in the sunlit portion of the vortex downstream of the region of PSCs (as inferred from HNO_3) and cold temperatures. The non-scanning measurements also showed increasing amounts of ClO after 21 Dec 1994 (Fig. 2b), as more of the observed area received sunlight.

Minimum 465 K temperatures were near the type II PSC threshold in early January, and remained low until late January when a series of strong warming events began. Throughout January, when MLS did not observe the Arctic (12), the vortex remained shifted well off the pole, and the unusually large region of low temperatures was mainly in sunlight. Thus it is expected that vortex ClO was considerably enhanced during January. MLS resumed Arctic measurements on 31 Jan 1995, when, as seen in the 3 Feb 1995 map (Fig. 1f), ClO was enhanced throughout the vortex. Temperatures rose near the type I PSC formation threshold in late January, and the deep cavity in HNO_3 was no longer apparent in early February (Fig. 1e). A small depression in HNO_3 was coincident with the 195 K temperature contour on 3 Feb 1995, and non-scanning measurements showed slightly deeper depressions on 5 to 7 Feb 1995, when it was somewhat colder; this may indicate that some HNO_3 was condensed in PSCs.

As noted above, minimum temperatures were below the type II PSC formation threshold during most of late December 1994, and through mid-January 1995. The presence of type II PSCs is an important factor in denitrification (the irreversible removal of HNO_3 by sedimentation of condensed particles) since the larger type II PSC particles, which also incorporate HNO_3 , are sedimented out at a faster rate than the smaller type I particles (22). Compared to late December, HNO_3 in the vortex was lower on all days with MLS measurements in February, including days when high minimum temperatures precluded PSC formation. Maximum values in early February were near 9.5 ppbv, as opposed to near

11.5 ppbv in late December. Since diabatic descent would be expected to increase HNO_3 over this period in the absence of other effects (16, 17), this suggests that some denitrification occurred. This decrease of ~ 2 ppbv was of similar magnitude to that seen in the Arctic between 22 Feb and 14 Mar 1993 (11), although actual values in March 1993 were higher, probably due to more transport from above in the early part of that winter. This is in contrast to a decrease of ~ 6 ppbv observed in the Antarctic over the same seasonal period (11). HNO_3 observed by MLS on 3 Feb 1995 was near 8.5 ppbv throughout most of the vortex; this can be contrasted with less than 6 ppbv observed throughout most of the vortex in the Antarctic spring (11).

A large decrease in 465 K vortex ozone was also seen between late December 1994 and early February 1995, and early February Arctic ozone (Fig. 2c) was considerably lower than in any of the previous three northern winters. The average rate of decrease between late 1 December and early February was similar to that in February and March 1993, with a net decrease in vortex-averaged ozone of -15 ± 7 in each period. Ozone abundances are larger inside the vortex than at lower latitudes at this level; diabatic descent is expected to bring in more ozone, but it is possible that dynamics could decrease ozone if low latitude air were entrained into the vortex. In February and March 1993, this possibility was ruled out by examination of passive tracer measurements from UARS(4). In the absence of passive tracer measurements with hemispheric coverage for the 1994-95 winter, trajectory calculations (16, 23) are used to examine transport processes. High resolution, domain-filling (24) trajectory calculations are used to investigate the possibility of intrusions of low-latitude air into the vortex, and a reverse trajectory procedure (23, 25) including diabatic motions is used to estimate changes in vortex-averaged ozone caused solely by (three-dimensional) transport. The trajectory calculations suggest no evidence for intrusion of low latitude air into the vortex before late January. The calculations do indicate intrusions in early February, but the computed vortex-averaged ozone decrease is no more than ~ 0.15 ppmv (Fig. 2c, open diamonds). An observed decrease between 1 and 8 Feb 1995 may

be partly due to such an intrusion. Three-dimensional transport processes are expected to cause ozone to increase slowly during late December (Fig. 2c, open triangles), with more rapid increases in late January and early February, when diabatic descent was enhanced during stratospheric warmings (16). These calculations show that, with only transport processes, 465 K vortex-averaged ozone in early February 1995 would have been near 3.0 to 3.3 ppmv, as opposed to the observed value of ~ 2.6 ppmv. This indicates that the decrease between 21 Dec 1994 and 1 Feb 1995 was caused mainly by chemical processing, and suggests that some chemical destruction was masked by air with more ozone descending to 465 K.

Lower stratospheric temperatures rose above the type IPSC threshold on about 8 Feb 1995 (Fig. 2a), but cooled again in late February and early March. ClO decreased rapidly after 8 Feb 1995, when temperatures increased (Fig. 2b). On 14 Feb 1995 (Fig. 1j), small regions of ClO greater than 1 ppbv were still seen in the vortex. The vortex had split at 465 K, and higher, vortex-like values of ClO, HNO₃ (Fig. 1i) and ozone (Fig. 1k) were seen in the small separated vortex over eastern Asia. Reverse domain-filling trajectory calculations initialized from observations on 8 Feb 1995 indicate that air from the vortex with enhanced ClO (as well as high HNO₃ and ozone) was drawn out into this region on 14 Feb 1995. ClO decreased further after 14 Feb 1995, but increased again when temperatures decreased in late February; by 8 Mar 1995 (Fig. 1n), ClO abundances in the vortex were similar to those on 14 Feb 1995. Trajectory calculations initialized on 28 Feb 1995 suggest that the air in the small region of enhanced ClO near 60°N, 100°E on 8 Mar 1995 came from a region of enhanced ClO in the vortex; since the small extra-vortex region probably represents only one MLS measurement profile, further analyses (26) would be necessary to determine whether or not it represents a real atmospheric feature.

After the decrease in early February, vortex-averaged lower stratospheric ozone remained nearly constant through the rest of the observing period. Because there was strong

wave activity in early February, diabatic descent was enhanced (16), and Lagrangian transport calculations for this period (Fig. 2c, open diamonds) suggest that vortex ozone would be expected to increase due to dynamics. That observed vortex-averaged ozone stayed relatively constant suggests that additional chemical depletion occurred. During the last few days of north-looking MLS measurements in this period, the highest ozone values were along the edge and outside the vortex (e. g., Fig. 1o); in such a situation, the vortex average becomes very sensitive to small changes in the position of high ozone with respect to the position of the PV contour used to define the vortex. Lagrangian transport calculations initialized on 28 Feb 1995 (open squares in Fig. 2c) suggest that most of the ozone change during 6 to 10 Mar 1995 can be explained by dynamical effects.

The evolution of column ozone (calculated above 100 hPa) over the observing period is also shown in Fig. 1. As expected from poleward and downward transport (27), maximum values increased between 21 Dec 1994 (Fig. 1 d) and 3 Feb 1995 (Fig. 1h). During the same period, minimum column ozone decreased by ~ 1 0% in the region of the lower stratospheric vortex. The magnitude of this decrease is consistent with that due to chemical depletion, since the lower stratospheric layer over which depletion was observed contributes $\sim 1/3$ of the column above 100 hPa. However, many dynamical factors also play a complex role in the evolution of column ozone (27, 28, 29) and more complete chemistry and transport models would be necessary to isolate the cause of this decrease. The morphology of the column ozone, with a region of low values in a confined area coincident with the lower stratospheric vortex (e.g., Fig. 1 p) is not in itself an indication of chemical depletion, as this morphology is typical of periods when low temperatures are located well inside the vortex (28); similar patterns were seen at times throughout the ~ 16 year record of Total Ozone Mapping Spectrometer data, including times when no chemical depletion was expected (28). Minimum column ozone values in the vortex region during the 1994-95 Arctic winter were somewhat lower than observed by MLS in the previous three winters (3, 10). Typical minimum values for Antarctic column ozone above 100 hPa observed by MLS

in September are less than 100 Dobson Units (DU) (3), in contrast to minimum values of ~ 200 DU shown here. Column ozone averaged from 60° to 80° N (not shown) increased between 21 Dec 1994 and 1 Feb 1995, due to the increase in maximum values. During February and early March, a slight downward trend was seen in this average, in contrast to previous years when MLS observed little or no trend in 60° to 80° N column ozone (10).

Figure 3 summarizes the spatial extent of observed ozone decreases and enhanced ClO. Figure 3a shows the ozone change between 21 Dec 1994 and 3 Feb 1995, displayed in PV/ θ -space (4, 17). The decrease in ozone over this period extended out to the vortex edge, and up to about 600 K (~ 25 km), with large decreases confined to the lowest levels shown, near 465 K. Figure 3b shows an average of the ClO on 1, 3 and 8 Feb 1995 (the days when MLS observed most enhancement) in PV/ θ -space; the region of enhanced ClO had nearly the same vertical extent as the region where ozone decreased, and extended almost out to the vortex edge at the lower levels. In the center of the vortex (at highest PV), ozone decreased by about 30% between late December 1994 and early February 1995, over 44 days. In February and March 1993, a maximum decrease of $\sim 20\%$ was seen over 35 days (4); the decrease in February and March 1993 was over a similar vertical range, but the largest decrease was away from the center of the vortex and at a higher altitude. Between 3 Feb 1995 and 10 March 1995, ozone at the highest PV at 465 K decreased an additional $\sim 5\%$, but small increases were seen at higher levels. A net decrease in ozone between 21 Dec 1994 and 10 Mar 1995 was seen only below ~ 500 K; this decrease was locally as much as $\sim 35\%$.

Arctic lower stratospheric temperatures in the 1994-95 winter were below the typical type I PSC formation threshold for ~ 3 months, longer than in any of the previous 16 years; the time spent below typical type I PSC formation temperatures (~ 35 days) was also longer than in any of those previous years (7). Consistent with the unusually low temperatures, enhanced ClO was observed in late December and throughout February and early March, and some denitrification, similar in magnitude to that seen in February and March 1993

(11), was inferred. The lower stratospheric chemical ozone depletion observed between late December 1994 and early February 1995 was as large or larger than the greatest previously reported decrease, which was in the 1992-1993 Arctic winter (4). Given the large degree of interannual variability in the Arctic winter, the predicted decreasing trend in lower stratospheric temperatures (30), and the continuing high levels of stratospheric chlorine (31), there is a potential for still greater ozone depletion during future Arctic winters.

REFERENCES AND NOTES

1. J.C. Farman, B.G. Gardiner, J. H. Shanklin, *Nature* 315, 207 (1985); R.S. Stolarski *et al.*, *ibid.* 322, 808 (1986).
2. M.B. McElroy and R.J. Salawitch, *Science* 243, 763 (1989); S. Solomon, *Nature* 347, 347 (1990); J.G. Anderson, D.W. Tooney, W.H. Brune, *Science* 251, 39 (1991).
3. J.W. Waters *et al.*, *Nature* 362, 597 (1993); J. W. Waters *et al.*, *Geophys. Res. Lett.* 20, 1219 (1993).
4. G.L. Manney *et al.*, *Nature* 370, 429 (1994).
5. J.W. Waters *et al.*, *Geophys. Res. Lett.*, in press (1995).
6. R.L. de Zafrá *et al.*, *Nature* 328, 408 (1987); J.G. Anderson, W.J. Brune, M.H. Proffitt, *J. Geophys. Res.* 94, 11,465 (1989); N. Larsen *et al.*, *Geophys. Res. Lett.* 21, 1611 (1994).
7. R. W. Zurek *et al.*, submitted to *Geophys. Res. Lett.*.
8. F.T. Barath *et al.*, *J. Geophys. Res.* 98, 10,751 (1993).
9. J. W. Waters, in *Atmospheric Remote Sensing by Microwave Radiometry*, M.A. Janssen, Ed. (Wiley, New York, 1993), chap. 8.
10. L. Froidevaux *et al.*, *J. Atmos. Sci.* 51, 2846 (1994).
11. M. L. Santee *et al.*, *Science* 267, 849 (1995).
12. During days when the MLS antenna was not performing a vertical scan, it was commanded to “track” the atmospheric limb at ~18 km tangent height; retrievals of ozone, ClO and HNO₃ on the 46 hPa pressure surface in the lower stratosphere are obtained from these “non-scanning” measurements, but with poorer vertical resolution than for scanning measurements.
13. The MLS pointing geometry and the inclination of the UARS orbit lead to measurement coverage from 80° latitude on one side of the equator to 34° on the other. The UARS

orbit plane precesses in such a way that all local solar times are sampled in about 36 days, after which the spacecraft is rotated 180° about its yaw axis. Jbus, 10 times per year MLS alternates between viewing northern and southern high latitudes. The time of each yaw maneuver is ~5 days earlier in each year than in the preceding year.

14. Potential temperature (θ) is defined as the temperature an air parcel would have if it were moved adiabatically to a pressure of 1000 hPa, and is related to pressure (p , in hPa) via $\theta = T(1000/p)^{0.286}$, where T is temperature in kelvin. Potential temperature is conserved under adiabatic conditions.
15. For large scale stratospheric motions, potential vorticity (PV) is defined as $PV = -g(f + \zeta)d\theta/dp$, where g is the acceleration due to gravity, f is the Coriolis parameter, p is pressure, θ is potential temperature (14), and ζ is the component of relative vorticity orthogonal to the θ surface. For adiabatic, frictionless flow, PV is conserved, and contours of PV on potential temperature surfaces are material lines. PV is calculated from United Kingdom Meteorological Office (UKM (.) assimilation model winds and temperatures (R. Swinbank and A. O'Neill, *Mon. Wea. Rev.* **122**, 686-702.)
16. G. I. Manney, R. W. Zurek, A. O'Neill, R. Swinbank, *J. Atmos. Sci.* **51**, 2973 (1994).
17. M. R. Schoeberl, L. R. Lait, P. A. Newman, J. E. Rosenfield, *J. Geophys. Res.* **97**, 7859 (1992).
18. From the UKMO analyses (15). US National Meteorological Center (NMC) temperatures are also available; for this time period, minimum vortex temperatures from NMC are typically 1-2 K lower than those from the UKMO (7).
19. R. J. Turco, O. B. Toon, P. Hamill, *J. Geophys. Res.* **94**, 16,493 (1989).
20. The region of enhanced ClO is highly localized in both horizontal and vertical directions, and a reasonable estimate of 465 K ClO can be made from the data obtained when the instrument was tracking the limb (13); this is not the case for ozone or HNO₃. An overall average offset of ~0.3 ppbv between ClO values from the non-scanning data and

the three-dimensional data has been added to the vortex average from non-scanning data for each day. This offset is attributed to the differing vertical resolutions for the two modes of operation.

21. D. Hanson and K. Mauersberger, *Geophys. Res. Lett.* **15**, 855 (1988).
22. O.B. Toon, R.P. Turco, P. Hamill, *Geophys. Res. Lett.* **17**, 445 (1990); R.J. Salawitch, G.J. Gobbi, S.C. Wofsy, M.B. McElroy, *Nature* **339**, 525 (1989).
23. Air parcels initialized throughout the stratosphere in one hemisphere are advected in three dimensions by a trajectory code (16), and are assigned mixing ratios of ozone based on observations on the initialization day; the calculation thus assumes that ozone mixing ratio is conserved (no chemical effects); G. L. Manney *et al.*, *J. Atmos. Sci.*, in press (1995); G. L. Manney *et al.*, submitted to *Geophys. Res. Lett.*.
24. "Domain-filling" calculations examine the evolution of many parcels (*60,000 are used here) initialized on an isentropic surface; A. O'Neill, W. L. Grose, V. D. Pope, H. Maclean, R. Swinbank, *J. Atmos. Sci.* **51**, 2800 (1994).
25. R. T. Sutton, H. Maclean, R. Swinbank, A. O'Neill, F. W. Taylor, *J. Atmos. Sci.* **51**, 2995 (1994).
26. M. R. Schoeberl *et al.*, *Geophys. Res. Lett.* **20**, 2861 (1993).
27. J. B. Rood, M. R. Schoeberl, *J. Geophys. Res.* **88**, 8491 (1983); D. G. Andrews, J. R. Holton, C. B. Leovy, *Middle Atmosphere Dynamics* (Academic Press, San Diego, 1987); M.-F. Wu, M. A. Geller, J. G. Olson, E. M. Larson, *J. Geophys. Res.* **92**, 3081 (1987); G. L. Manney, L. Froidevaux, J. W. Waters, R. W. Zurek, *J. Geophys. Res.* **100**, 2953 (1995).
28. W. J. Randel and F. Wu, *Geophys. Res. Lett.* **22**, in press (1995).
29. R. B. Rood, *Pure Appl. Geophys.* **121**, 1049 (1983); K. K. Tung and H. Yang, *J. Geophys. Res.* **93**, 12,537 (1988); H. Yang, E. Olaguer, J. K. Tung, *J. Atmos. Sci.*

- 48, 442 (1991); A. Y. Hou, H. R. Schneider, M. K. W. Ko, *J. Atmos. Sci.* 48, 547 (1991).
30. J. K. Angell, *J. Clim.*, 1, 1296 (1988); R. Rind, R. Suozzo, N. K. Balachandran, M. J. Prather, *J. Atmos. Sci.* 47, 475 (1990); J. Austin, N. Butchart, K. P. Shine, *Nature* 360, 221 (1992).
31. M. J. Prather and R. L. Watson, *Nature* 344, 729 (1990); F. S. Rowland, *Annu. Rev. Phys. Chem.* 42, 731 (1991).
32. ClO abundances are much smaller on the "night" side of the orbit, due to a lack of photolysis of the dimer Cl₂O₂, formed from ClO recombination. Other species are also shown for the "day" side of the orbit to be consistent with ClO.
33. We thank the members of the MLS team for their assistance and support, especially T. Lungu and I. Nakamura. We also thank T. Luu for data management; J. Sabutis and W. J. Randel for helpful discussions. This work was performed at the Jet Propulsion Laboratory, California Institute of Technology under contract with the National Aeronautics and Space Administration.

FIGURE LEGENDS

Fig. 1. Maps of MLSHNO_3 (ppbv), ClO (ppbv), and ozone (ppmv) mixing ratios interpolated onto the 465 K potential temperature (14) surface using UKMO temperatures (15), and column ozone (DU) above 100 hPa in late December 1994 and February and March 1995. The maps are polar orthographic projections extending to the equator, with the Greenwich meridian at the bottom and dashed black circles at 30°N and 60°N . They were produced by linear interpolation of all measurements taken on the "day" side of the orbit (32) over a 24-hour period. The two black contours on each mixing ratio plot are potential vorticity (PV) (10^5), calculated from UKMO temperature and wind fields. The outer contour is $0.25 \times 10^4 \text{ Km}^2 \text{ kg}^{-1} \text{ s}^{-1}$, the inner contour $0.30 \times 10^4 \text{ Km}^2 \text{ kg}^{-1} \text{ s}^{-1}$. The magenta contours on the HNO_3 maps show UKMO temperatures of 195 and 190 K. The white circle on the ClO maps indicates the edge of polar night.

Fig. 2. (a) Minimum UKMO temperatures (18) in the vortex region (as defined by the $0.25 \times 10^4 \text{ Km}^2 \text{ kg}^{-1} \text{ s}^{-1}$ PV contour) on the 465 K isentropic surface (14); (b) and (c) vortex-averaged mixing ratios, calculated by dividing the area integral of the mixing ratio inside the $0.25 \times 10^4 \text{ Km}^2 \text{ kg}^{-1} \text{ s}^{-1}$ PV contour (the outermost contour in Fig. 1) by the area enclosed by that contour, of (b) ClO (ppbv) and (c) ozone (ppmv) at 465 K. MLS data on the "day" side of the orbit arc used (32). The thin green line shows the 1991-1992 winter, the thin blue line the 1992-1993 winter and the thin red line the 1993-1994 winter; observations in the 1994-1995 winter are represented by thick black lines and solid black symbols. The dashed black line in (b) shows the vortex-averaged ClO estimated from single-layer data (12, 20). The large gap in MLS data during January in each year is when MLS is observing the southern hemisphere (13). open symbols in (c) show Lagrangian transport calculations initialized on 21 Dec 1994 (triangles), 1 Feb 1995 (diamonds) and 28 Feb 1995 (squares).

Fig. 3. (a) Change in ozone mixing ratio (ppmv) between 21 Dec 1994 and 3 Feb 1995, as a function of PV and θ (4, 17), in the lower to mid-stratosphere. In order to conveniently view a vertical section, PV is scaled to give a similar range of values throughout the θ domain shown (4, 16, 17) and is in “vorticity” units of 10^{-4} s^{-1} (16). (b) Time-averaged ClO (ppbv) in the same domain, for 1, 3, and 8 Feb 1995, the days on which MLS observed most enhancement of ClO (Fig. 2b). MLS data from the “day” side of the orbit arc used (32). The PV contour used for the vortex averages in Fig. 2 corresponds to a scaled PV value of $1.2 \times 10^{-4} \text{ s}^{-1}$ (16). The zero contour in (a) is outlined in white. The nearly vertical black lines indicate the approximate location of the vortex edge.

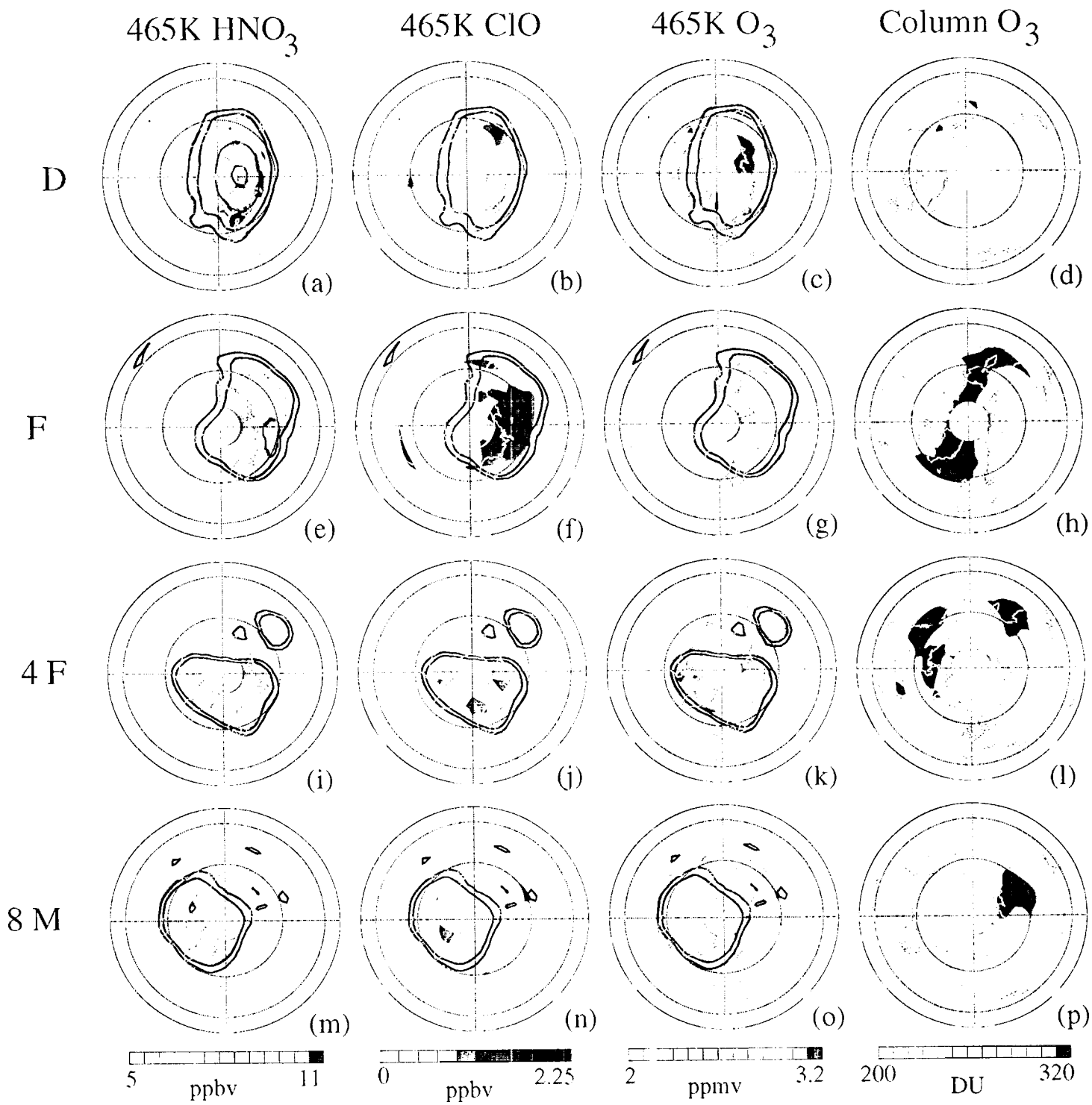


Figure 1

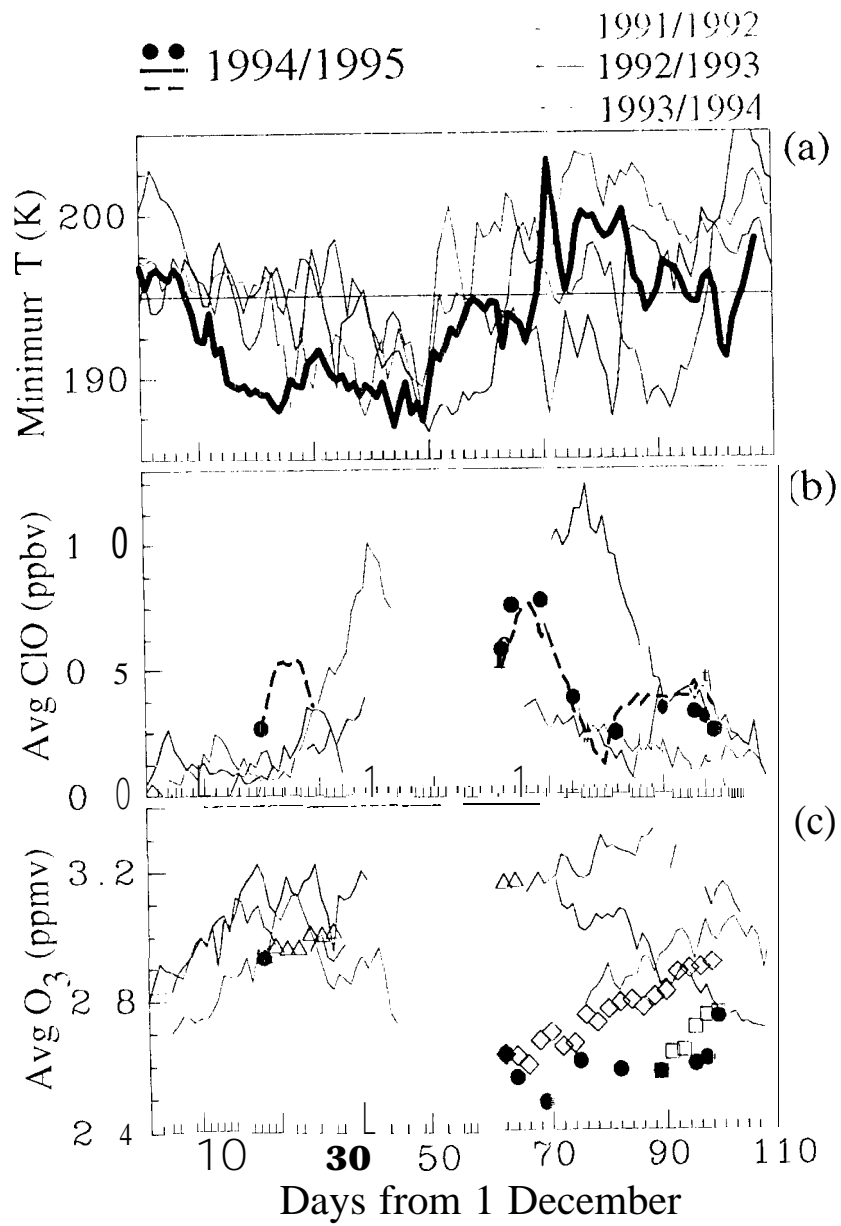


Figure 2

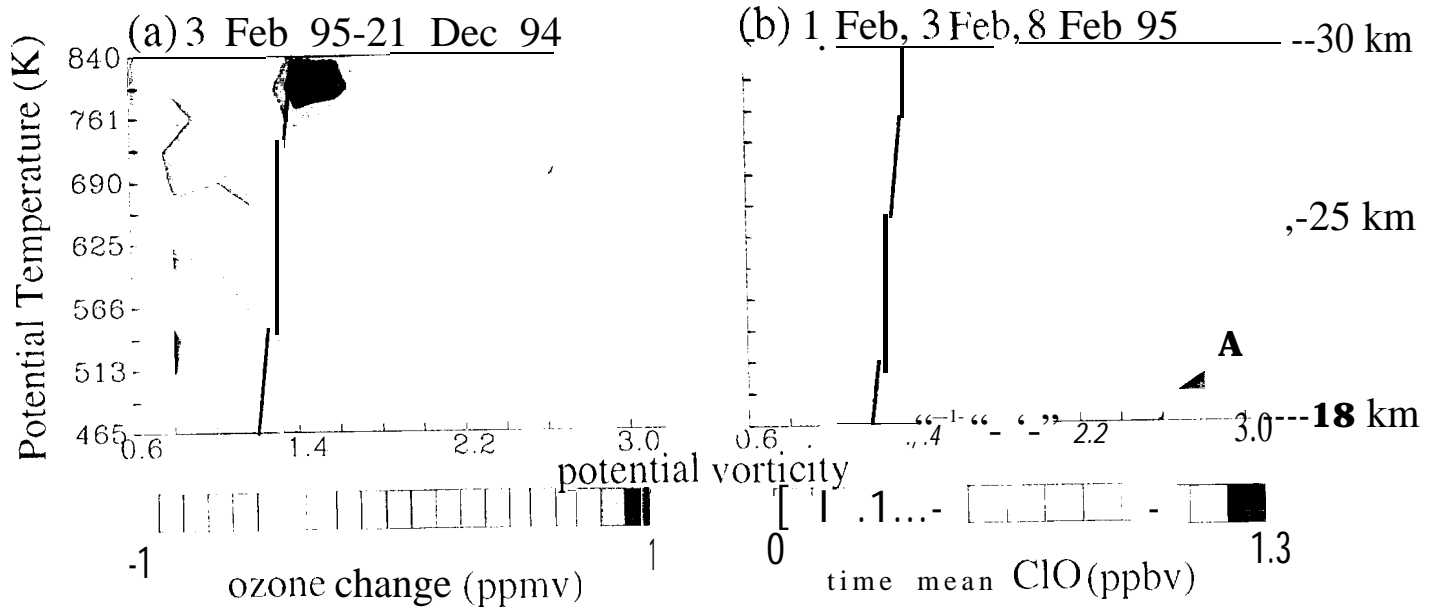


Figure 3